

GRAVITATIONAL WAVES FROM ISOLATED NEUTRON STARS^a

E. GOURGOULHON, S. BONAZZOLA

*Département d'Astrophysique Relativiste et de Cosmologie,
UPR 176 C.N.R.S.,
Observatoire de Paris,
F-92195 Meudon Cedex, France*

Continuous wave gravitational radiation from isolated rotating neutron stars is discussed. The general waveform and orders of magnitude for the amplitude are presented for various known pulsars. The specific case of gravitational radiation resulting from the distortion induced by the stellar magnetic field is presented. Finally some preliminary results about the signal from the whole population of neutron stars in the Galaxy are discussed.

1 Introduction

As compact objects with significant internal velocities, neutron stars constitute a priori valuable gravitational wave sources. Besides catastrophic events such as their coalescence¹ or their gravitational collapse², these stars can be interesting sources of continuous wave gravitational radiation, provided they deviate from axisymmetry. Whereas the accompanying lecture³ focuses on mechanisms, such as spontaneous symmetry breaking, which imply accretion from a companion, the present lecture is devoted to radiation from isolated rotating neutron stars.

2 General considerations

2.1 A general formula for gravitational emission by a rotating star

When dealing with neutron stars, the classical *weak-field* quadrupole formula for gravitational wave generation is not valid. For highly relativistic bodies, Iper⁴ has shown that the leading term in the gravitational radiation field h_{ij} is given by a formula which is structurally identical to the quadrupole formula for weak-field sources⁵, the Newtonian quadrupole being simply replaced by Thorne's quadrupole moment⁶ \mathcal{I}_{ij} . The non-axisymmetric deformation of neutron stars being very tiny, the total Thorne's quadrupole can be linearly

^ato appear in the Proceedings of the International Conference on Gravitational Waves: Sources and Detectors, Cascina (Pisa), Italy — March 19-23, 1996 (World Scientific, in press).

decomposed into the sum of two pieces: $\mathcal{I}_{ij} = \mathcal{I}_{ij}^{\text{rot}} + \mathcal{I}_{ij}^{\text{dist}}$, where $\mathcal{I}_{ij}^{\text{rot}}$ is the quadrupole moment due to rotation and $\mathcal{I}_{ij}^{\text{dist}}$ is the quadrupole moment due to the process that distorts the star, for example an internal magnetic field⁷, anisotropic stresses from the nuclear interactions or irregularities in the solid crust⁸. Let us make the assumption that the distorting process has a privileged direction, i.e. that two of the three eigenvalues of $\mathcal{I}_{ij}^{\text{dist}}$ are equal. Let then α be the angle between the rotation axis and the principal axis of $\mathcal{I}_{ij}^{\text{dist}}$ which corresponds to the non-degenerate eigenvalue. The two modes h_+ and h_\times of the gravitational radiation field in a transverse traceless gauge derived from the Thorne-Ipser quadrupole formula are⁷

$$h_+ = h_0 \sin \alpha \left[\frac{1}{2} \cos \alpha \sin i \cos i \cos \Omega t - \sin \alpha \frac{1 + \cos^2 i}{2} \cos 2\Omega t \right] \quad (1)$$

$$h_\times = h_0 \sin \alpha \left[\frac{1}{2} \cos \alpha \sin i \sin \Omega t - \sin \alpha \cos i \sin 2\Omega t \right], \quad (2)$$

where i is the inclination angle of the “line of sight” with respect to the rotation axis and

$$h_0 = \frac{16\pi^2 G}{c^4} \frac{I \epsilon}{P^2 r}, \quad (3)$$

where r is the distance of the star, $P = 2\pi/\Omega$ is the rotation period of the star, I its moment of inertia with respect of the rotation axis and $\epsilon := -3/2 \mathcal{I}_{zz}^{\text{dist}}/I$ is the *ellipticity* resulting from the distortion process.

It may be noticed that Eqs. (1)-(3) are structurally equivalent to Eq. (1) of Zimmermann & Szedenits⁹, although this latter work is based on a different physical hypothesis (Newtonian precessing *solid* star).

From formulæ (1)-(2), it appears clearly that there is no gravitational emission if the distortion axis is aligned with the rotation axis ($\alpha = 0$ or π). If both axes are perpendicular ($\alpha = \pi/2$), the gravitational emission is monochromatic at twice the rotation frequency. In the general case ($0 < |\alpha| < \pi/2$), it contains two frequencies: Ω and 2Ω . For small values of α the emission at Ω is dominant. Numerically, Eq. (3) results in the amplitude

$$h_0 = 4.21 \times 10^{-24} \left[\frac{\text{ms}}{P} \right]^2 \left[\frac{\text{kpc}}{r} \right] \left[\frac{I}{10^{38} \text{ kg m}^2} \right] \left[\frac{\epsilon}{10^{-6}} \right]. \quad (4)$$

Note that $I = 10^{38} \text{ kg m}^2$ is a representative value for the moment of inertia of a $1.4 M_\odot$ neutron star. In the following, I is systematically set to this value.

The values of h_0 resulting from Eq. (4) are given in Table 1 for two young rapidly rotating pulsars (Crab and Vela), the nearby pulsar Geminga¹⁰ and

Table 1: Gravitational wave amplitude h_0 on Earth as a function of the ellipticity ϵ for five pulsars.

name	rotation period P [ms]	distance r [kpc]	GW amplitude h_0
Crab	33	2	$1.9 \times 10^{-27}(\epsilon/10^{-6})$
Vela	89	0.5	$1.1 \times 10^{-27}(\epsilon/10^{-6})$
Geminga	237	0.16	$4.7 \times 10^{-28}(\epsilon/10^{-6})$
PSR B1957+20	1.61	1.5	$1.1 \times 10^{-24}(\epsilon/10^{-6})$
PSR J0437-4715	5.76	0.14	$9.1 \times 10^{-25}(\epsilon/10^{-6})$

two millisecond pulsars: the second^b fastest one, PSR 1957+20, and the nearby millisecond pulsar PSR J0437-4715¹¹. At first glance, millisecond pulsars seem to be much more favorable candidates than the Crab or Vela. However, in Table 1, ϵ is in units of 10^{-6} and the very low value of the period derivative \dot{P} of millisecond pulsars implies that their ellipticity is at most 2×10^{-9} , as we shall see in § 2.3.

2.2 Detectability by VIRGO

Let us give a crude estimate of the minimum amplitude h_0 detectable by the VIRGO interferometer. Whereas the expected amplitude is very weak, as compared with other astrophysical processes such coalescences or gravitational collapses, one can take advantage of the permanent character of the signal to increase the signal-to-noise ratio by increasing the observing time. Indeed for an integration time T , the signal-to-noise ratio reads

$$\frac{S}{N} = \frac{h_0}{\tilde{h}(f)} \sqrt{T}, \quad (5)$$

where $\tilde{h}(f)$ is VIRGO sensitivity (square root of the noise spectral density) at the frequency f . The minimum values of h_0 leading to $S/N = 1$ when $T = 3$ yr are given in Table 2. In view of these values, we shall take as a basis for our discussion that *in order to be detectable by VIRGO, a rotating neutron star must produce $h_0 > 10^{-26}$.*

^bthe “historical” millisecond pulsar PSR 1937+21, which is the fastest one, is not considered for it is more than twice farther away.

Table 2: Minimal amplitude h_0 detectable ($S/N = 1$) by VIRGO within 3 years of integration. The values of $\tilde{h}(f)$ have been taken from Giazzoto et al.¹²

frequency f [Hz]	sensitivity \tilde{h} [Hz ^{-1/2}]	detectable amplitude min h_0
10	10^{-21}	10^{-25}
30	10^{-22}	10^{-26}
100	3×10^{-23}	3×10^{-27}
1000	3×10^{-23}	3×10^{-27}

Table 3: Absolute upper bounds on the ellipticity and the GW amplitude derived from the measured spin-down rate of pulsars.

name	GW frequencies		max. ellipticity	max. GW amplitude
	f [Hz]	$2f$ [Hz]	ϵ_{\max}	$h_{0,\max}$
Vela	11	22	1.8×10^{-3}	1.9×10^{-24}
Crab	30	60	7.5×10^{-4}	1.4×10^{-24}
Geminga	4.2	8.4	2.3×10^{-3}	1.1×10^{-24}
PSR B1509-68	6.6	13.2	1.4×10^{-2}	5.8×10^{-25}
PSR B1706-44	10	20	1.9×10^{-3}	4.2×10^{-25}
PSR B1957+20	621	1242	1.6×10^{-9}	1.7×10^{-27}
PSR J0437-4715	174	348	2.9×10^{-8}	2.6×10^{-26}

2.3 Upper bounds on gravitational radiation from pulsars

An absolute upper bound on h_0 can be derived by assuming that the observed slowing down of the pulsar (the so-called \dot{P}) is entirely due to the energy carried away by gravitational radiation. Let us stress that this is not a realistic assumption since most of the \dot{P} is thought to result instead from losses via electromagnetic radiation and/or magnetospheric acceleration of charged particles — at least for Crab-like pulsars. However, this provides an upper bound on the ellipticity ϵ and the gravitational wave amplitude h_0 . The resulting values are given in Table 3. The five first entries in this Table correspond to the five highest values of $h_{0,\max}$ among the 706 pulsars of the catalog by Taylor et al.^{13,14}.

New et al.¹⁵ have recently pointed out that if the mean ellipticity of pulsars is taken to be of the order of the ϵ_{\max} of millisecond pulsars, i.e. $\epsilon \sim 10^{-9}$ (cf.

Table 4: Minimum values of the ellipticity required to produce $h_0 = 10^{-26}$ on Earth.

name	min ϵ
Crab	$5.3 \times 10^{-6} = 7 \times 10^{-3} \epsilon_{\max}$
Vela	$9.1 \times 10^{-6} = 5 \times 10^{-3} \epsilon_{\max}$
Geminga	$2.1 \times 10^{-5} = 9 \times 10^{-3} \epsilon_{\max}$
PSR B1957+20	$9.1 \times 10^{-9} > \epsilon_{\max}$
PSR J0437-4715	$1.1 \times 10^{-8} = 0.4 \epsilon_{\max}$

Table 3), then the Crab pulsar reveals to be a much worse candidate than PSR B1957+20, as it can be seen by setting $\epsilon = 10^{-9}$ in Table 1: $h_0^{\text{Crab}} \simeq 2 \times 10^{-30}$ versus $h_0^{1957+20} \simeq 10^{-27}$.

2.4 Ellipticity required for a detectable amplitude

Given the threshold $h_0 = 10^{-26}$ for detectability by the VIRGO interferometer (§ 2.2), one can consider the corresponding value of ϵ resulting from Eq. (4) and compare it with the maximum value given by the pulsar slowing down (Table 3). The results are presented in Table 4. From that it can be concluded that an ellipticity as small as 10^{-8} leads to a detectable amplitude for the nearby millisecond pulsar PSR J0437-4715, whereas the Crab or Vela pulsar should have an ellipticity of the order 10^{-5} , which is about one percent of the maximum allowable ellipticity as given by the spin-down rate (§ 2.3).

3 The specific case of magnetic field induced distortion

In this section, we consider the specific example when the distortion results from the neutron star's magnetic field. In this case the ellipticity is expressible as $\epsilon = \beta \mathcal{M}^2 / \mathcal{M}_0^2$, where \mathcal{M} is the magnetic dipole moment, $\mathcal{M}_0 = 2.6 \times 10^{32} \text{ A m}^2$ and β a dimensionless coefficient which measures the efficiency of the magnetic structure in distorting the star. For an incompressible fluid Newtonian body endowed with a uniform magnetic field¹⁶, $\beta = 1/5$. For a given pulsar, \mathcal{M} can be inferred from the value of $P\dot{P}$.

We have developed a numerical code to compute the deformation of magnetized neutron stars within general relativity^{7,17}. The solutions obtained are fully relativistic and self-consistent, all the effects of the electromagnetic field on the star's equilibrium (Lorentz force, spacetime curvature generated by the electromagnetic stress-energy) being taken into account. The magnetic field is axisymmetric and poloidal.

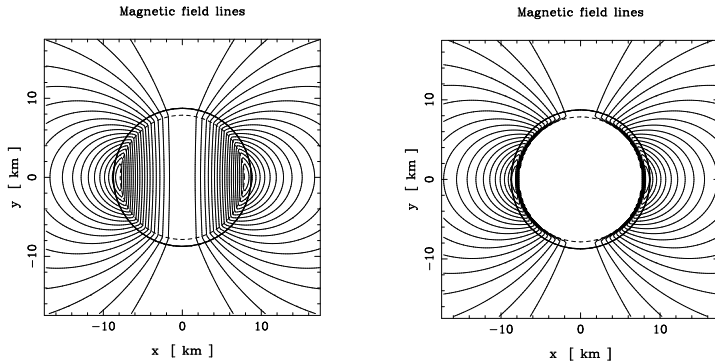


Figure 1: Magnetic field lines generated by a current distribution localized in the crust of the star (left) or exterior to a type I superconducting core (right). The thick line denotes the star's surface and the dashed line the internal limit of the electric current distribution (left) and the external limit of the superconducting region (right). The distortion factor corresponding to these configurations is $\beta = 8.84$ (left) and $\beta = 157$ (right).

The reference (non-magnetized) configuration is taken to be a $1.4 M_{\odot}$ static neutron star built with the equation of state UV₁₄+TNI of Wiringa, Fiks & Fabrocini¹⁸. Various magnetic field configurations have been considered; the most representative of them are presented hereafter.

Let us first consider the case of a perfectly conducting interior (normal matter, non-superconducting). The simplest magnetic configuration compatible¹⁷ with the MHD equilibrium of the star results in electric currents in the whole star with a maximum value at half the stellar radius in the equatorial plane. The computed distortion factor is $\beta = 1.01$, which is above the $1/5$ value of the uniform magnetic field/incompressible fluid Newtonian model⁷ but still very low. Another situation corresponds to electric currents localized in the neutron star crust only. Figure 1 presents one such configuration: the electric current is limited to the zone $r > r_* = 0.9 r_{\text{eq}}$. The resulting distortion factor is $\beta = 8.84$.

In the case of a superconducting interior, of type I (which means that all magnetic field has been expelled from the superconducting region), the distortion factor somewhat increases. In the configuration depicted in Fig. 1, the neutron star interior is superconducting up to $r_* = 0.9 r_{\text{eq}}$. For $r > r_*$, the matter is assumed to be a perfect conductor carrying some electric current. The resulting distortion factor is $\beta = 157$. For $r_* = 0.95 r_{\text{eq}}$, β is even higher: $\beta = 517$.

The above values of β , of the order $10^2 - 10^3$, though much higher than

in the simple normal case, are still too low to lead to an amplitude detectable by the first generation of interferometric detectors in the case of the Crab or Vela pulsar, which would require ⁷ $\beta > 10^4$. It is clear that the more disordered the magnetic field the higher β , the extreme situation being reached by a stochastic magnetic field: the total magnetic dipole moment \mathcal{M} almost vanishes, in agreement with the observed small value of \dot{P} , whereas the mean value of B^2 throughout the star is huge. Note that, according to Thompson & Duncan ¹⁹, turbulent dynamo amplification driven by convection in the newly-born neutron star may generate small scale magnetic fields as strong as 3×10^{11} T with low values of B_{dipole} outside the star and hence a large β . In order to mimic such a stochastic magnetic field, we have considered the case of counter-rotating electric currents. The resulting distortion factor can be as high as $\beta = 5.7 \times 10^3$.

If the neutron star interior forms a type II superconductor, the magnetic field inside the star is organized in an array of quantized magnetic flux tubes, each tube containing a magnetic field $B_c \sim 10^{11}$ T. As discussed by Ruderman ²⁰, the crustal stresses induced by the pinning of the magnetic flux tubes is of the order $B_c B / 2\mu_0$, where B is the mean value of the magnetic field in the crust ($B \sim 10^8$ T for typical pulsars). This means that the crust is submitted to stresses $\sim 10^3$ higher than in the uniformly distributed magnetic field (compare $B_c B / 2\mu_0$ with $B^2 / 2\mu_0$). The magnetic distortion factor β should increase in the same proportion. We have not done any numerical computation to confirm this but plan to study type II superconducting interiors in a future work.

4 Gravitational radiation background from the whole population of neutron stars in the Galaxy

4.1 The squared signal

Let N be the total number of neutron stars in our Galaxy. The response of an interferometric detector to the gravitational wave field (h_+^i, h_\times^i) [cf. Eqs. (1)-(2)] emitted by the i^{th} neutron star is

$$h_i(t) = F_+^i(t) h_+^i(t) + F_\times^i(t) h_\times^i(t) , \quad (6)$$

where $F_+^i(t)$ and $F_\times^i(t)$ are beam-pattern factors which depend on the direction of the star with respect to the detector arms. They vary with time because of the Earth rotation and revolution around the Sun. This results in an amplitude modulation ^{21,7} as well as a Doppler shift ^{22,23} of the signal. The time-average of the total (i.e. the sum on all the galactic neutron stars) is zero but not the

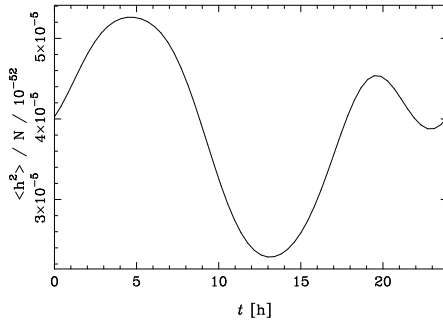


Figure 2: Total squared signal (divided by N) from a distribution of N neutron stars concentrated in the galactic disk with a height scale of 0.5 kpc. The average rotation period is assumed to be $\bar{P} = 5$ ms and the mean ellipticity $\bar{\epsilon} = 10^{-8}$.

time-average of the *squared* total signal:

$$\langle h^2 \rangle = \frac{1}{\tau} \int_{t_0}^{t_0+\tau} \left[\sum_{i=1}^N h_i(t) \right]^2 dt . \quad (7)$$

The key-point is that if the galactic neutron star distribution is not isotropic, $\langle h^2 \rangle$ will exhibit temporal variation, with a period of one sidereal day. The precise shape of the signal depends on the neutron star distribution. An example²⁴ corresponding to a disk distribution is presented in Fig. 2.

It can be shown²⁴ that the signal-to-noise ratio for detecting this signal is

$$\frac{S}{N} = \frac{\langle h^2 \rangle}{2\tilde{h}^2} \left(\frac{T}{2\Delta\nu} \right)^{1/2} , \quad (8)$$

where $\Delta\nu$ is the frequency bandwidth and T is the observation time. It appears that such a signal might be detected if the number of neutron stars falling in the frequency range of the VIRGO detector is larger than $\sim 10^6 - 10^7$.

4.2 Number of rapidly rotating neutron stars in the Galaxy

From the star formation rate and the outcome of supernova explosions, the total number of neutron stars (NS) in the Galaxy has been estimated^{25–26} to be about 10^9 . The number of *observed* NS is much lower than this number: ~ 700 NS are observed as radio pulsars^{13–14}, ~ 150 as X-ray binaries, among

which ~ 30 are X-ray pulsars^{27–28}, and a few as isolated NS, through their X-ray emission²⁹.

For our purpose, the relevant number is given by the fraction of these $\sim 10^9$ NS which rotates sufficiently rapidly to emit gravitational waves in the frequency bandwidth of VIRGO-like detectors. Putting the low frequency threshold of VIRGO to $f_{\min} = 5$ Hz (optimistic value!), and using the fact that the highest gravitational frequency of a star which rotates at the frequency f is $2f$ (cf. § 2.1), this means the rotation period of a detectable NS must be lower than $P_{\max} = 0.4$ s. The NS that satisfy to this criterion can be divided in three classes: (C1) young pulsars which are still rapidly rotating (e.g. Crab or Vela pulsars); (C2) millisecond pulsars, which are thought to have been spun up by accretion when being a member member of a close binary system (during this phase the system may appear as a low-mass X-ray binary); (C3) NS with $P < 0.4$ s which do not exhibit the pulsar phenomenon.

The number of millisecond pulsars in the Galaxy is estimated³⁰ to be of the order $N_2 \sim 10^5$. The number of *observed* millisecond pulsars ($P < 10$ s) is about 50 and is continuously increasing.

The number of young (non-recycled) rapidly rotating NS is more difficult to evaluate. An estimate can be obtained from the fact that the observed non-millisecond pulsars with $P < 0.4$ s represent 28 % of the number of catalogued pulsars and that the total number of active pulsars in the Galaxy is around 5×10^5 . The number of rapidly rotating non-recycled pulsars obtained in this way is $N_1 \sim 1.4 \times 10^5$.

Adding N_1 and N_2 gives a number of $\sim 2 \times 10^5$ NS belonging to the populations (C1) and (C2) defined above. This number can be considered as a lower bound for the total number of NS with $P < 0.4$ s. The final figure depends on the number of members of the population (C3). This latter number is (almost by definition!) unknown. All that can be said is that it is lower than the total number of NS in the Galaxy ($\sim 10^9$).

Acknowledgments

This work has benefited from discussions with F. Bondu, A. Giazotto, P. Haensel, P. Hello and S.R. Valluri.

References

1. Blanchet L., this volume.
2. Stark R.F., Piran T., *Phys. Rev. Lett.* **55**, 891 (1985).
3. Bonazzola S., Gourgoulhon E., this volume.

4. Ipser J.R., *Astrophys. J.* **166**, 175 (1971).
5. Misner C.W., Thorne K.S., Wheeler J.A., *Gravitation* (Freeman, New York, 1973).
6. Thorne K.S., *Rev. Mod. Phys.* **52**, 299 (1980).
7. Bonazzola S., Gourgoulhon E., *Astron. Astrophys.*, in press (preprint: astro-ph/9602107).
8. Haensel P., in *Astrophysical Sources of Gravitational Radiation (Les Houches 1995)*, eds. J.-A. Marck, J.-P. Lasota, to be published.
9. Zimmermann M., Szedenits E., *Phys. Rev. D* **20**, 351 (1979).
10. Caraveo P.A., Bignami G.F., Mignani R., Taff L.G., *Astrophys. J.* **461**, L91 (1996)
11. Johnston S. et al., *Nature* **361**, 613 (1993).
12. Giazzoto A. et al., in *First Edoardo Amaldi Conference on Gravitational Wave Experiments*, eds. E. Cocchia, G. Pizzella, F. Ronga (World Scientific, Singapore, 1995).
13. Taylor J.H., Manchester R.N., Lyne A.G., *Astrophys. J. Suppl.* **88**, 529 (1993).
14. Taylor J.H., Manchester R.N., Lyne A.G., Camilo F., unpublished work (1995).
15. New K.C.B., Chanmugam G., Johnson W.W., Tohline J.E., *Astrophys. J.* **450**, 757 (1995).
16. Gal'tsov D.V., Tsvetkov V.P., Tsirulev A.N., *Zh. Eksp. Teor. Fiz* **86**, 809 (1984); English translation in *Sov. Phys. JETP* **59**, 472 (1984).
17. Bocquet M., Bonazzola S., Gourgoulhon E., Novak J., *Astron. Astrophys.* **301**, 757 (1995).
18. Wiringa R.B., Fiks V., Fabrocini A., *Phys. Rev. C* **38**, 1010 (1988).
19. Thompson C., Duncan R.C., *Astrophys. J.* **408**, 194 (1993).
20. Ruderman M., *Astrophys. J.* **382**, 576 (1991).
21. Jotania K., Dhurandhar S.V., *Bull. Astr. Soc. India* **22**, 303 (1994)
22. Jotania K., Valluri S.R., Dhurandhar S.V., *Astron. Astrophys.* **306**, 317 (1996)
23. Grave X. et al., this volume.
24. Bonazzola S., Gourgoulhon E., Giazzoto A., in preparation.
25. Timmes F.X., Woosley S.E., Weaver T.A., *Astrophys. J.* **457**, 834 (1996).
26. Pacini F., this volume.
27. White N.E., Nagase F., Parmar A.N., in *X-ray binaries*, eds. Lewin W.H.G., van Paradijs J., van den Heuvel E.P.J. (Cambridge University Press, Cambridge, 1995).
28. van Paradijs J., in *The lives of the neutron stars*, eds. Alpar M.A., Kiziloglu Ü., van Paradijs J. (Kluwer Academic Publishers, Dordrecht,

- 1995).
29. Walter F.M., Wolk S.J., Neuhäuser R., *Nature* **379**, 233 (1996).
 30. Bhattacharya D., in *X-ray binaries*, eds. Lewin W.H.G., van Paradijs J., van den Heuvel E.P.J. (Cambridge University Press, Cambridge, 1995).